View metadata, citation and similar papers at core.ac.uk

brought to you by CORE

provided by NASA Technical Reports Server

DEVELOPMENT OF THE PROGRAM

SPECEL

A SPECIAL ELEMENT FOR ELASTO-PLASTIC

CRACK TIP ANALYSIS

(NASA-CR-140895) DEVELOPMENT OF THE PROGRAM SPECEL: A SPECIAL ELEMENT FOR ELASTO-PLASTIC CRACK TIP ANALYSIS (Carnegie Inst. of Tech.) 32 p HC $3.75 CSCL 20K

N75-15073

Unclas

G3/39 06649

J. L. Swedlow

Report SM 74-10

December 1974

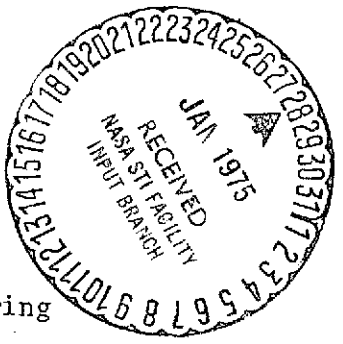

Department of Mechanical Engineering
Carnegie Institute of Technology
Pittsburgh, Pennsylvania

INTRODUCTION

RATIONALE FOR YET ANOTHER ELEMENT

The discipline known as fracture mechanics has evolved over the last half-century from A. A. Griffith's famous results to the present situation of testing standards, advocacy of competing fracture criteria, and potent--and sometimes conflicting--methods for experimentation and analysis. All this work has the common characteristics that first, the presence of a sharp macro-crack is presumed, and second, that there is a region of some small but finite radius surrounding the crack tip to which we are virtually blind. While it is true that various researches have over the years reduced the size of this region, the fact remains that we know very little of what happens at the crack tip. Of that which we do know, e.g., 'slipping-off' mechanisms, void growth, stress and strain 'singularities' and so on, it has proven quite difficult to translate such information into a more comprehensive and therefore useful form. In particular, our experimentally-based information currently outstrips theoretical insight; this discrepancy prompts the present effort.

What is intended here is to devise means for an improved articulation of the analysis of elasto-plastic flow in the vicinity of a crack tip or, for that matter, any sharp re-entrant corner. This is to be done through the development of a 'special crack-tip element' to be used in conjunction with finite element analysis. The element must accomodate those models of displacement associated with a crack without at the same time presuming any additional features of the behavior which cannot *a priori* be proven. There is thus required a certain economy in the formulation for we are constrained to a minimum of input and seek a maximum of output.

We cannot, for example, be limited solely to elastic behavior as characterizes the work of Byskov [1], Wilson [2], among others. Nor may we begin with 'fully plastic' behavior as done, say, by Hilton [3] following the work of Hutchinson [4], and Rice and Rosengren [5]. While both of these limit cases have their usefulness, the fact that they are limit cases precludes information on the *process* whereby the material goes from one to the other. Even the work by Tracey [6], which attempts to include both, bypasses the issue of process and blinds us to the rate, means, and conditions for the material's transition from purely elastic to fully plastic response.

At the present, it appears that sufficient capability and information are in hand to proceed along the lines envisaged at the outset of this effort. A fair amount of experience with and theoretical understanding of the theory of elasto-plastic flow has been accumulated so that new means of problem-solving may be employed. And, we have enough insight, hopefully, into crack behavior to begin practicing the economy outlined above. Some steps in this direction have now been taken, and this report outlines the formulation, progress to date, and the next steps to be made.

CONTEXT

ELASTO-PLASTICITY IN PLANE STRAIN

The theory of elasto-plastic flow has been elucidated fully elsewhere (see, e.g., [7]), so that we need only transcribe relations pertinent to our present interest. The theory is stated in terms of increments of displacement and stress, and of instantaneous or accumulated values of stress. The equilibrium equations, in the absence of body forces, are

$$\partial\delta\sigma_x/\partial x + \partial\delta\tau_{xy}/\partial y = 0$$

$$\partial\delta\tau_{xy}/\partial y + \partial\delta\sigma_y/\partial y = 0 \qquad (1)$$

and the constitutive relations for plane strain are written as

$$2\mu\left(1 + \beta s_z^2\right)\delta\varepsilon_x = \left[1 - \nu + \beta\left(s_x^2 + 2\nu s_x s_z + s_z^2\right)\right]\delta\sigma_x + \left[-\nu + \beta\left(s_x s_y - 2\nu s_z^2\right)\right]\delta\sigma_y + 2\left[\beta\left(s_x + \nu s_z\right) s_{xy}\right]\delta\tau_{xy}$$

$$2\mu\left(1 + \beta s_z^2\right)\delta\varepsilon_y = \left[-\nu + \beta\left(s_y s_x - 2\nu s_z^2\right)\right]\delta\sigma_x + \left[1 - \nu + \beta\left(s_y^2 + 2\nu s_y s_z + s_z^2\right)\right]\delta\sigma_y + 2\left[\beta\left(s_y + \nu s_z\right)s_{xy}\right]\delta\tau_{xy} \qquad (2)$$

$$\mu\left(1 + \beta s_z^2\right)\delta\gamma_{xy} = \left[\beta s_{xy}\left(s_x + \nu s_z\right)\right]\delta\sigma_x + \left[\beta s_{xy}\left(s_y + \nu s_z\right)\right]\delta\sigma_y + \left\{1 + 2\beta\left[s_{xy}^2 + (1 + \nu)s_z^2\right]\right\}\delta\tau_{xy}$$

with the inverse

$$\delta\sigma_x/E = \left[(\lambda + 2\mu)/E - s_x^2/(1 + 1/\beta)\right]\delta\varepsilon_x + \left[\lambda/E - s_x s_y/(1 + 1/\beta)\right]\delta\varepsilon_y - \left[s_x s_{xy}/(1 + 1/\beta)\right]\delta\gamma_{xy}$$

$$\delta\sigma_y/E = \left[\lambda/E - s_y s_x/(1 + 1/\beta)\right]\delta\varepsilon_x + \left[(\lambda + 2\mu)/E - s_y^2/(1 + 1/\beta)\right]\delta\varepsilon_y - \left[s_y s_{xy}/(1 + 1/\beta)\right]\delta\gamma_{xy} \qquad (3)$$

$$\delta\tau_{xy}/E = -\left[s_{xy} s_x/(1 + 1/\beta)\right]\delta\varepsilon_x - \left[s_{xy} s_y/(1 + 1/\beta)\right]\delta\varepsilon_y + \left[\mu/E - s_{xy}^2/(1 + 1/\beta)\right]\delta\gamma_{xy}$$

In (2) and (3), $\delta\varepsilon_x = \partial\delta u/\partial x$; $\delta\varepsilon_y = \partial\delta v/\partial y$; $\delta\gamma_{xy} = \partial\delta u/\partial y + \partial\delta v/\partial x$; μ is the elastic shear modulus; ν is Poisson's ratio; $E = 2(1 + \nu)\mu$ is Young's modulus; $\lambda = 2\nu\mu/(1 - 2\nu)$ is Lamé's constant; β is the ratio of the elastic shear modulus to the slope of the octahedral stress-octahedral plastic strain

curve, i.e., $\beta = \mu/\mu_o^{(p)}$ and must be non-negative and bounded; and

$$s_x = (2\sigma_x - \sigma_y - \sigma_z)/(3\sqrt{3}\tau_o)$$

$$s_y = (2\sigma_y - \sigma_z - \sigma_x)/(3\sqrt{3}\tau_o)$$

$$s_z = (2\sigma_z - \sigma_x - \sigma_y)/(3\sqrt{3}\tau_o)$$

$$s_{xy} = \tau_{xy}/(\sqrt{3}\tau_o)$$

with

$$\tau_o^2 = (2/9)(\sigma_x^2 + \sigma_y^2 + \sigma_z^2 - \sigma_y\sigma_z - \sigma_z\sigma_x - \sigma_x\sigma_y + 3\tau_{xy}^2)$$

Inserting (3) into (1) and replacing $\delta\varepsilon_x$, $\delta\varepsilon_y$, $\delta\gamma_{xy}$ by their equivalents in terms of gradients of the displacement increments yields two quasi-linear partial differential equations for δu, δv. Boundary conditions may be written in terms of these displacement increments or the traction increments δt_x, δt_y which are obtained by using (3) with Cauchy's relations.

Alternatively, one may arrive at a problem statement through use of an analogue to the theorem of minimum potential energy. If we define

$$\begin{aligned}\Pi = (E/2)\int_A \Big\{ &\Big[(\lambda + 2\mu)/E - s_x^2/(1 + 1/\beta)\Big]\delta\varepsilon_x^2 - 2\Big[s_y s_{xy}/(1 + 1/\beta)\Big]\delta\varepsilon_y\delta\gamma_{xy} \\ &+ \Big[(\lambda + 2\mu)/E - s_y^2/(1 + 1/\beta)\Big]\delta\varepsilon_y^2 - 2\Big[s_x s_{xy}/(1 + 1/\beta)\Big]\delta\varepsilon_x\delta\gamma_{xy} \\ &+ \Big[\mu/E - s_{xy}^2/(1 + 1/\beta)\Big]\delta\gamma_{xy}^2 + 2\Big[\lambda/E - s_x s_y/(1 + 1/\beta)\Big]\delta\varepsilon_x\delta\varepsilon_y\Big\} dA \\ &- \int_{S_t} (\delta t_x \delta u + \delta t_y \delta v)\, dS\end{aligned}$$

where S_t is that portion of the boundary S on which traction increments are specified, then an extremum of Π (actually a minimum) leads to an equivalent result. This approach is germane to any finite element formulation, in that the final stiffness equations develop most naturally by minimizing the functional Π. In the case at hand, this procedure is used in a direct manner as described in the next section.

DETAILS

ELEMENT FORMULATION AND PROGRAM STRUCTURE

At the crack tip, we consider an array of sectors which together comprise a special element. Each sector is connected to a regular finite element, in the present instance a constant-strain or linear-displacement element. In Figure 1a, we show a particular grouping of sectors and regular elements, and this arrangement has been used in the computations described below. In Figure 1b, we show details for a typical sector. It occupies the space $0 < r < 2r_e$, $\theta_1 < \theta < \theta_2$ as shown; has nodes at (r_e, θ_1), $(2r_e, \theta_1)$, $(2r_e, \theta_2)$, (r_e, θ_2), and $(0, \theta)$, usually referred to in that order; and has a displacement field given in terms of cartesian (u,v) or circular (u_r, v_θ) components. It is convenient always to write coordinates in terms of (r, θ) rather than (x, y).

The cartesian components of the displacement vector are taken to be

$$\begin{aligned} u &= Ar\cos\theta + Cr\sin\theta + (E + F\theta)r^p \cos\theta - (G + H\theta)r^q \sin\theta + u_o \\ v &= Br\sin\theta + Dr\cos\theta + (E + F\theta)r^p \sin\theta + (G + H\theta)r^q \cos\theta + v_o \end{aligned} \tag{5}$$

and the corresponding cylindrical components are obtained from

$$u_r = u\cos\theta + v\sin\theta$$

$$v_\theta = -u\sin\theta + v\cos\theta$$

so that

$$\begin{aligned} u_r &= Ar\cos^2\theta + Br\sin^2\theta + Cr\sin\theta\cos\theta + Dr\sin\theta\cos\theta + \\ &\quad + (E + F\theta)r^p + u_o\cos\theta + v_o\sin\theta \end{aligned}$$

$$\begin{aligned} v_\theta &= -Ar\sin\theta\cos\theta + Br\sin\theta\cos\theta - Cr\sin^2\theta + Dr\cos^2\theta \\ &\quad + (G + H\theta)r^q - u_o\sin\theta + v_o\cos\theta \end{aligned}$$

where A, B,..., H are coefficients to be determined; p, q are exponents to be found; and u_o, v_o are rigid translations of the element. In

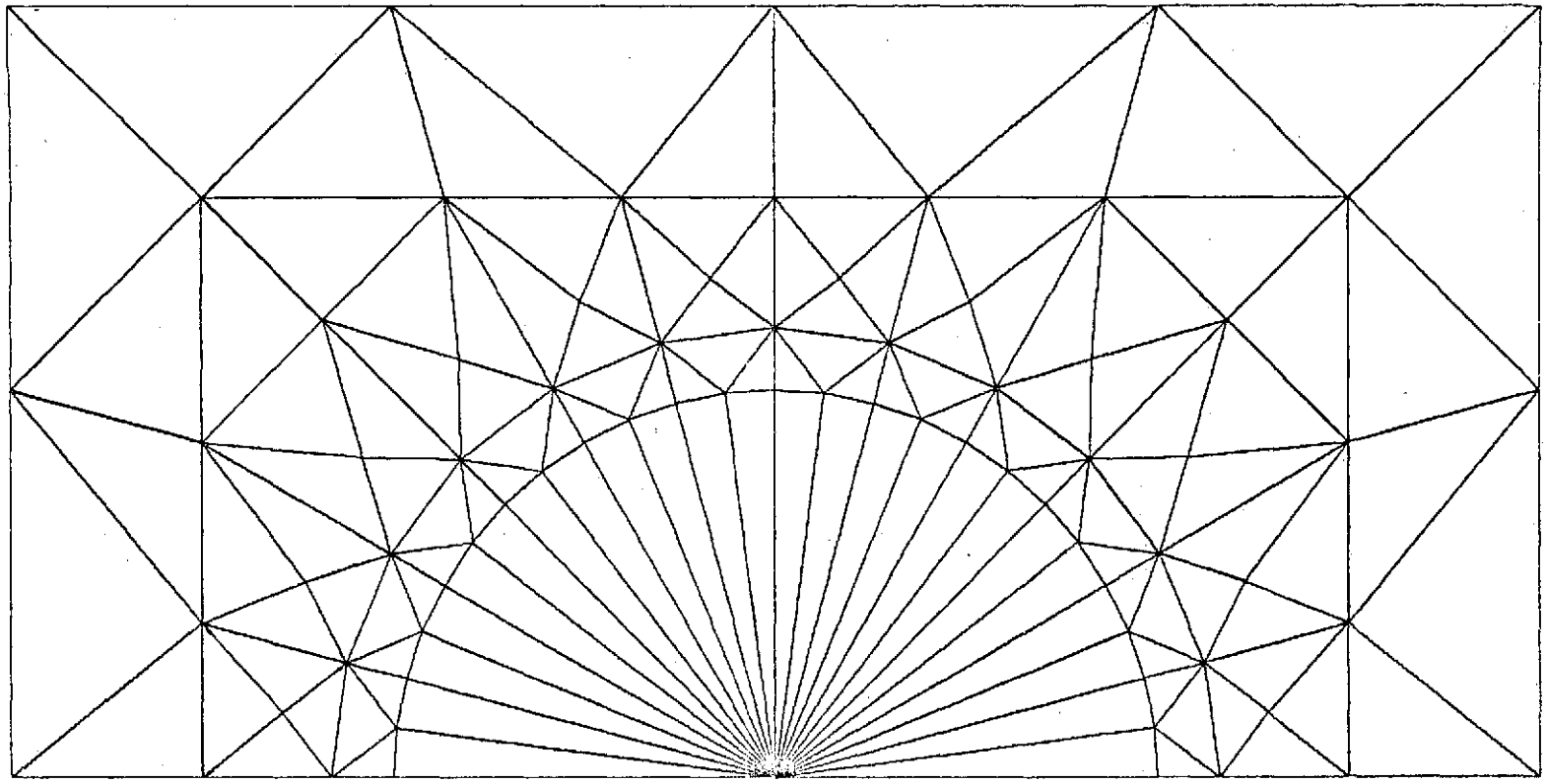

Figure 1a - Array of sectors comprising special element, connected to regular elements

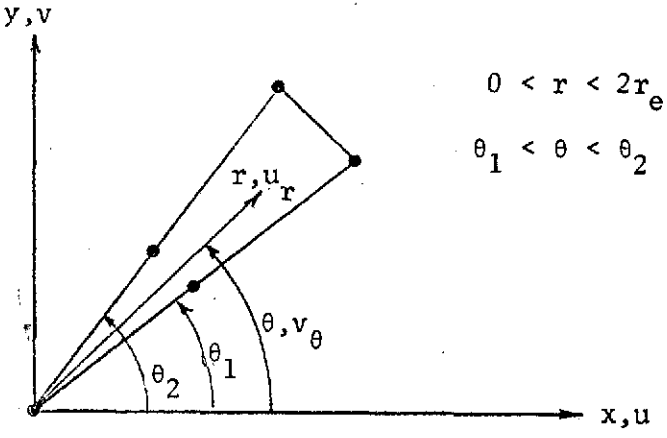

Figure 1b - A typical sector of the special element

addition, (D - C)/2 is a rigid rotation about the origin in Figure 1b. In addition, we may note from (5) that A, B give uniform normal strains in cartesian coordinates, and that D + C gives a uniform shear. To the extent that p, q ≠ integer*, then, terms governed by E, F and G, H represent the special aspect of the element. The first pair plus the exponent p relate to radial motion, as is evident in (6), and the second pair plus q concern circumferential motion.

Obviously, more complex functions than those shown in (5) or (6) may be set up to represent the displacement field within the sector. One could add, for example, quadratic and even cubic terms to (5), or the expressions in (5) or (6) may be replaced by isoparametric [8] forms following, say, Barsoum [9]. The present objective, however, is not so much achievement of high accuracy in the detailed modelling of crack-tip behavior; rather our intent is to make sure that a certain approach to the problem works at all. Thus, use of a simple displacement field seems warranted at the present stage of development. In keeping with the economy of formulation noted at the outset, we observe that the expressions in (5) or (6) possess the minimal attributes of rigid motion, uniform strain, and the special feature we seek to establish [8].

The next step in formulation is to replace the coefficients A, B, ..., H in (5) and (6) by their equivalent in terms of nodal point displacements. We therefore construct a vector of nodal displacements, referred to the cartesian coordinate directions, as

$$\{\underline{u}^T\} = \{u_1\ v_1\ u_2\ v_2\ u_3\ v_3\ u_4\ v_4\ u_5\ v_5\} \tag{7}$$

---

*Note that $0 < p,q < 1$ is the operating range of interest.

In (7), superscript T denotes transpose. The order of nodal numbering begins, as indicated above, at (r_e, θ_1) and continues counterclockwise to r = 0. Then, using the vector

$$\{\underline{A}^T\} = \{A\ B\ C\ D\ E\ F\ G\ H\ u_o\ v_o\} \tag{8}$$

we may write (5) at each of the five nodal positions to arrive at a set of ten equations of the form

$$\{\underline{u}\} = [Q]\ \{\underline{A}\} \tag{9}$$

where [Q] is a 10 × 10 matrix whose elements depend on nodal point coordinates. Inversion of (9) leads to

$$\{\underline{A}\} = [Z]\ \{\underline{u}\} \tag{10}$$

Then (5) may be replaced by

$$\begin{Bmatrix} u\ (r,\theta) \\ v\ (r,\theta) \end{Bmatrix} = [\alpha(r,\theta)]\ \{\underline{u}\} \tag{5'}$$

and (6) by

$$\begin{Bmatrix} u_r(r,\theta) \\ v_\theta(r,\theta) \end{Bmatrix} = [\gamma(r,\theta)]\ \{\underline{u}\} \tag{6'}$$

where $[\alpha(r,\theta)]$ and $[\gamma(r,\theta)]$ are 2 × 10 matrices whose elements depend upon nodal coordinates and position of reference within the sector. Finally, we may differentiate (5') to obtain a vector of strains, viz.

$$\{\varepsilon\} = \begin{Bmatrix} \varepsilon_x \\ \varepsilon_y \\ \gamma_{xy} \end{Bmatrix} = [\beta(r,\theta)]\ \{\underline{u}\} \tag{11}$$

and $[\beta(r,\theta)]$ is a 3 × 10 matrix.* Elements in the pertinent matrices listed above appear in the Appendix.

In the same manner that the strain-displacement relations are transformed from total or accumulated values, to incremental values, we may

---

*The matrix [β] in (11) is distinct from the modulus ratio in (2) and (3).

alter (5') and (11) for use in elasto-plasticity. Thus, if the increments of displacement at nodal points may be formed into a vector $\{\delta\underline{u}\}$ in the pattern of (7), the displacement increments interior to a sector are given by

$$\begin{Bmatrix}\delta u\ (r,\theta)\\ \delta v\ (r,\theta)\end{Bmatrix} = [\alpha(r,\theta)]\ \{\delta\underline{u}\} \tag{12}$$

Furthermore, the strain increments are written as

$$\{\delta\varepsilon\} = \begin{Bmatrix}\delta\varepsilon_x(r,\theta)\\ \delta\varepsilon_y(r,\theta)\\ \delta\gamma_{xy}(r,\theta)\end{Bmatrix} = [\beta(r,\theta)]\ \{\delta\underline{u}\} \tag{13}$$

and the matrices $[\alpha(r,\theta)]$ and $[\beta(r,\theta)]$ are the same as given in (5') and (11), and as detailed in the Appendix.

We introduce next a vector of stress increments as

$$\{\delta\sigma\} = \begin{Bmatrix}\delta\sigma_x(r,\theta)\\ \delta\sigma_y(r,\theta)\\ \delta\tau_{xy}(r,\theta)\end{Bmatrix} \tag{14}$$

and, from (3), it follows that

$$\{\delta\sigma\} = [M]\ \{\delta\varepsilon\} \tag{15}$$

where [M] is a symmetric 3 × 3 matrix whose elements depend upon the accumulated or instantaneous stresses, the elastic constants, and slope of the octahedral stress-octahedral plastic strain curve. Association of (3) and (15) indicates that

$$M_{11} = \lambda + 2\mu - s_x^2\, E/(1 + 1/\beta)$$

$$M_{22} = \lambda + 2\mu - s_y^2\, E/(1 + 1/\beta)$$

$$M_{33} = \mu - s_{xy}^2 E/(1 + 1/\beta)$$

$$M_{12} = M_{21} = \lambda - s_x s_y E/(1 + 1/\beta)$$

$$M_{23} = M_{32} = - s_y s_{xy} E/(1 + 1/\beta)$$

$$M_{31} = M_{13} = - s_x s_{xy} E/(1 + 1/\beta)$$

and the definitions of the various terms remain as stated in the previous section.

The functional in the integral theorem cited above now takes the form, for one sector,

$$\Pi_s = \frac{1}{2} \int_{\theta_1}^{\theta_2} \int_0^{2r_e} \{\delta\varepsilon^T\} [M] \{\delta\varepsilon\} \, r dr d\theta - \{\delta\underline{T}^T\} \{\delta\underline{u}\}$$

or

$$\Pi_s = \frac{1}{2} \{\delta\underline{u}\} \int_{\theta_1}^{\theta_2} \int_0^{2r_e} [\beta^T(r,\theta)] [M] [\beta(r,\theta)] \, r dr d\theta \{\delta\underline{u}\} - \{\delta\underline{T}^T\} \{\delta\underline{u}\} \qquad (16)$$

in which $\{\delta\underline{T}\}$ is a vector of nodal forces in an order that corresponds to that used in constructing $\{\delta\underline{u}\}$--see (7).

At this stage, the normal next step is to require that Π be stationary, with respect to nodal displacement increments, and the result is a linear relation between $\{\delta\underline{u}\}$ and $\{\delta T\}$ viz,

$$[K_s] \{\delta\underline{u}\} = \{\delta T\} \qquad (17)$$

where, for the sector,

$$[K_s] = \int_{\theta_1}^{\theta_2} \int_0^{2r_e} [\beta^T(r,\theta)] [M] [\beta(r,\theta)] \, r dr d\theta$$

While the same sort of result obtains in the present case, two additional relations must be developed. That is, we must determine conditions in p and q, as used in (5) or (6), from suitable manipulation of Π. Let us suppose, for example, that each sector has its own values of p and q. Then, in addition to (17), we must require

$$\partial\Pi_s/\partial p = 0, \qquad \partial\Pi_s/\partial q = 0$$

It may be shown, however, that this supposition leads to incompatibilities between adjacent sectors of the special element, to the extent that p and q vary from one sector to the next. Hence, in a formal sense, it is preferable to define

$$\Pi_e = \sum_{s=1}^{n} \Pi_s \tag{18}$$

where n is the total number of sectors in the special element. Then, letting p and q be common to all sectors, we require that

$$\partial \Pi_e / \partial p = 0, \qquad \partial \Pi_e / \partial q = 0 \tag{19}$$

which gives the additional relations needed.

The foregoing gives a useful clue to tactics for problem solving, and a variety of alternatives may be listed. Let us suppose that expressions of the form (16) are summed via (18); to that total, we add values of Π_r for all m regular elements surrounding the special element, viz:

$$\Pi = \sum_{s=1}^{n} \Pi_s + \sum_{r=1}^{m} \Pi_r \tag{20}$$

The final value Π is evidently quadratic in the nodal displacement increments throughout the domain modelled for a given problem and horribly non-quadratic in the exponents p and q in the special element. Because the overall problem is thus non-quadratic, one could approach its solution by attempting to minimize Π (in (20)) directly. This has the advantage of being notionally straightforward; it is at the same time quite expensive because algorithms for achieving extremal values are operationally slow when large numbers of variables are being treated.

Alternatively, we may utilize the fact that most of the variables in (20) appear in quadratic form. Writing the symbolic expression

$$d\Pi = (\partial\Pi/\partial\{\delta u\})d\{\delta u\} + (\partial\Pi/\partial p)dp + (\partial\Pi/\partial q)dq = 0$$

where $\{\delta u\}$ (in contrast to $\{\delta \underline{u}\}$) is the set of all nodal displacement increments in the domain of interest, we observe that a sufficient condition for the solution is

$$\begin{aligned} \partial\Pi/\partial\{\delta u\} &= [K]\ \{\delta u\} - \{\delta T\} = 0 \\ \partial\Pi/\partial p &= \partial\Pi_e/\partial p = 0 \\ \partial\Pi/\partial q &= \partial\Pi_e/\partial q = 0 \end{aligned} \qquad (21)$$

In (21), [K] is the master stiffness matrix for the domain, $\{\delta T\}$ is the set of all nodal force increments, and the first relation is thereby a set of linear algebraic relations for $\{\delta u\}$ in terms of $\{\delta T\}$, the latter presumably known. The second and third relations, however, are each single non-linear algebraic equations governing p and q. All three of (21) must be satisfied simultaneously.

Using this alternative approach, we have constructed a computer program SPECEL for the special element embedded in an array of regular elements. Its basic procedure for the kth increment may be outlined simply as follows. The increment begins by setting p and q to the values obtained from the previous increment and, using these values, a set of stiffness equations is set up. Thus the first of (21) is solved. The energy-like term Π_e is found and minimized with respect to p and q, that is, the exponents are adjusted to effect the second and third of (21). With these new values of p and q the stiffness equations are re-solved. This process is repeated until a minimum of Π itself is established so that (21) is satisfied. The results are then processed in the usual manner [10], checking to see that any unloading is taken properly into account, computing and printing various items of information such as displacements,

stresses, and the J-integral. A flow chart is given in Figure 2.

At the present writing, an exception to the foregoing procedure is programmed for the first load increment. Since this step is wholly elastic, the exponents are pre-set to precisely one-half (0.5) and no searching is performed to find 'better' values, i.e., values which would reduce Π_e. This exception stems from efforts to verify performance of the code by comparing it to known elastic solutions; we have yet to decide whether to retain this feature or, through a trivial change in code, force the first increment into the same pattern as obtains for subsequent load steps.

STATUS

ELASTIC AND INITIAL PLASTIC RESPONSE

Having written code to implement the formulation described above, the next step was to check it out in some detail. It happens that, although the bulk of the formulation involves the concepts expressed in the preceeding section, the bulk of the code itself involves the details of matrices such as those given in the Appendix and their manipulation. Thus verification can and did go forward in terms of elastic analysis, i.e., using the constant terms in [M] given in (15) et seq.

Using both the element arrays shown in Figures 1a and 3, a sequence of problems was solved. The first set involved uniform tension and uniform extension of the two maps. Results of these analyses indicated some errors in the code which were then corrected. What was determined ultimately is that the special feature of the element creates a low noise level in the sector's force vector; the singular terms are active, in effect, even though excitation is solely uniaxial homogeneous stress.

Figure 2 - Flow chart for SPECEL

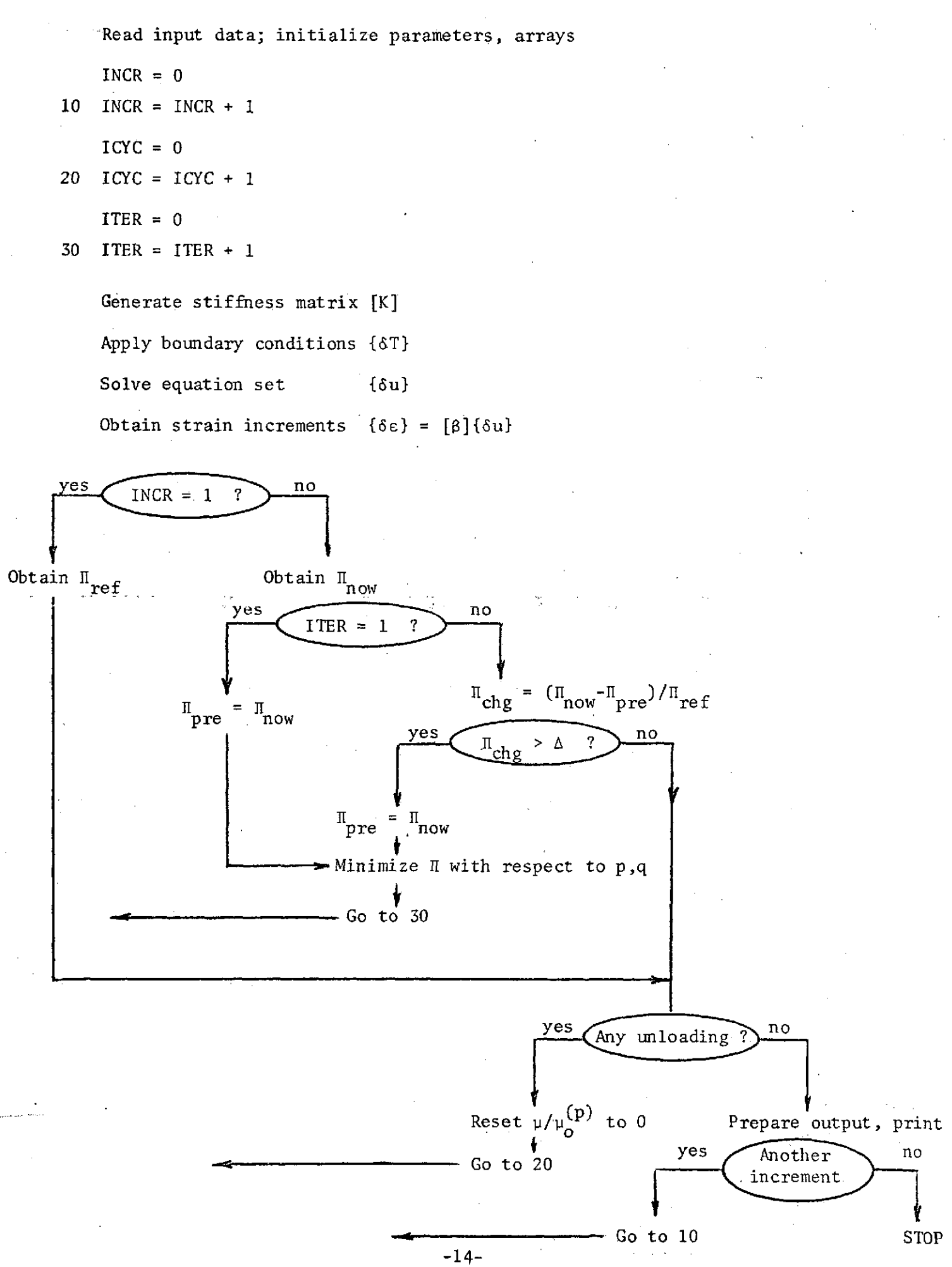

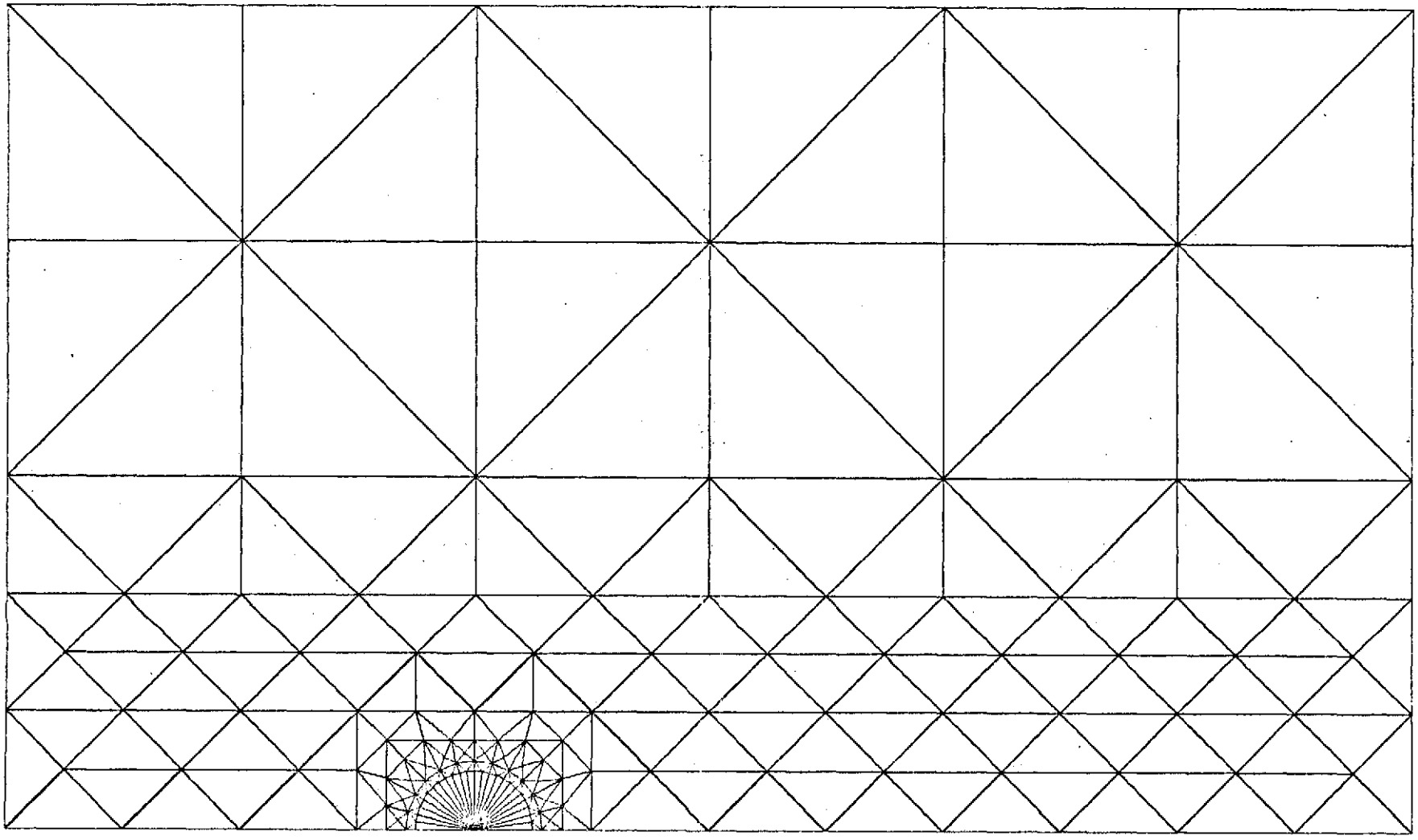

Figure 3 - Special element embedded in a larger array of regular elements

The magnitude of resultant noise is, however, quite low. If, for example, the applied stress is $\bar{\sigma}$ and $\bar{\sigma}r_e = 28125$, the noise level nowhere exceeds 0.32% of this amount when 24 sectors are used in the special element. This effect was examined in some detail. We find that it is predictable in terms of the formulation (5), that it is of the order of Δ^2 (where $\Delta = \theta_2 - \theta_1$), and that it is not an objectionable result of the simple representation (5) of a complex situation.

Moving next to crack problems, the map in Figure 3 was then subjected to two loadings. The first is uniaxial tension of a cracked panel, where the crack length/ligament length ratio is 1/2. For that case, the conventional stress intensity is given [11] as

$$K_I = 3.17\ \bar{\sigma}\sqrt{a}$$

where a is the crack length, here set to unity. The computation gave an average value of J over seven paths, which when converted to K_I, is

$$K_I = 3.122\ \bar{\sigma}\sqrt{a}$$

and the coefficient of variation of K_I is 0.0090. Thus the error in stress intensity is about 1.5% and the variation* is about 0.9% over circular paths having radii ranging from 0.0032 to 0.1218. (It may be noted that crack length is 1 and that the special element radius is 0.125.) This result is regarded as satisfactory.

The second loading imposed on the range of Figure 3 may be termed a 'pure' K_I excitation. At all boundary nodes except those along the flank of the crack, it was required that

---

*The sample coefficient of variation is the standard deviation divided by the average.

$$u = \sqrt{(2r)} \times 10^{-2} \times (5/3 - \cos\theta)\cos\theta/2$$
$$v = \sqrt{(2r)} \times 10^{-2} \times (5/3 - \cos\theta)\sin\theta/2 \qquad (22)$$

The values above result if $E = 10^7$ lb/in^2, $\nu = 1/3$, $K_I = 1.5\sqrt{\pi} \times 10^5$ lb/in$^{3/2}$, and the problem is in plane strain. Using the procedure outlined above to obtain K_I, a value of $1.5363\sqrt{\pi} \times 10^5$ lb/in$^{3/2}$ was achieved, the coefficient of variation being 0.92%. The error in K_I is seen to be 2.42% which, we believe, is explicable as follows. A complex (i.e., non-homogeneous) excitation is transmitted from the outer boundary to the special element via regular elements. The latter are known to be slightly stiffer than the continuum they represent so that, in the present instance, the loading on the special element will exceed the precise amount. We observe here that the excess is modest, and we expect that this pattern will be reflected in the computed nodal point displacements relative to the exact solution as given in (22). As seen in Figures 4 and 5, such is the case. Moreover, we observe that the circumferential behavior of the displacements is quite accurate and, in terms of nodal displacements for the special element, response is quite satisfactory.

Stresses interior to the element are also acceptable. In Figures 6 and 7 we plot the principal stresses which may be derived from (22) as

$$\sigma_1 = 1.5 \times 10^5 \times \sqrt{(a/2r)} \times (1 + \sin\theta/2)\ \cos\theta/2$$
$$\sigma_2 = 1.5 \times 10^5 \times \sqrt{(a/2r)} \times (1 - \sin\theta/2)\ \cos\theta/2 \qquad (23)$$

Values derived from (23) are given in Figures 6 and 7 for three values of r/a, along the midline of each sector. It is seen that the stresses tend to be high but not by an amount that greatly exceeds the original overloading through amplification of K_I. Moreover, the circumferential gradient is well replicated except where the stresses approach null values

Figure 4 - Horizontal displacement, normalized, for pure K_I loading at remote boundary as a function of angular position--nodal point values. $K_I = 1.5\sqrt{\pi} \times 10^5 \text{lb/in}^{3/2}$, $r_e/a = 0.06250$, $\nu = 1/3$, $E = 10^7 \text{lb/in}^2$, plane strain.

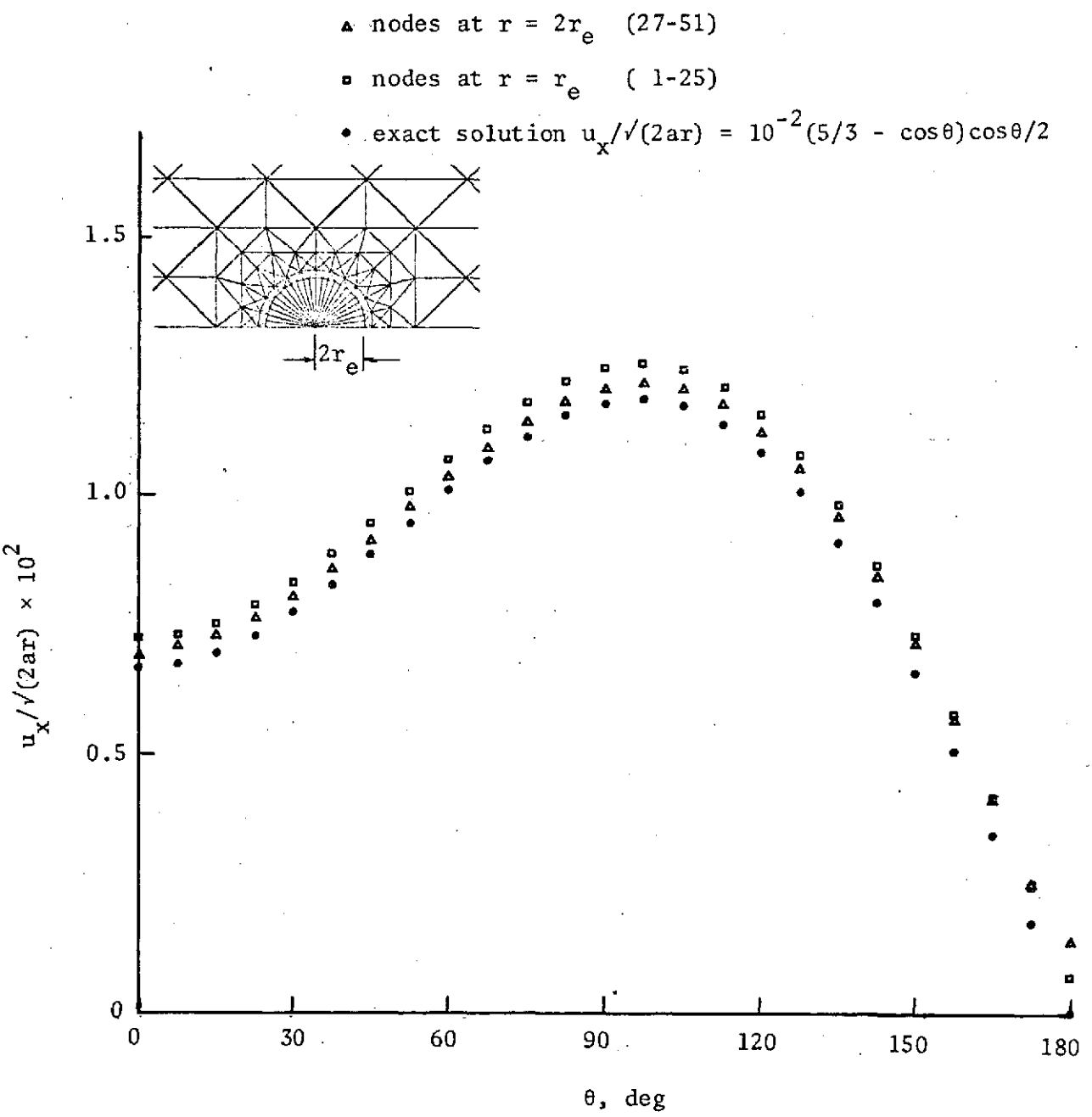

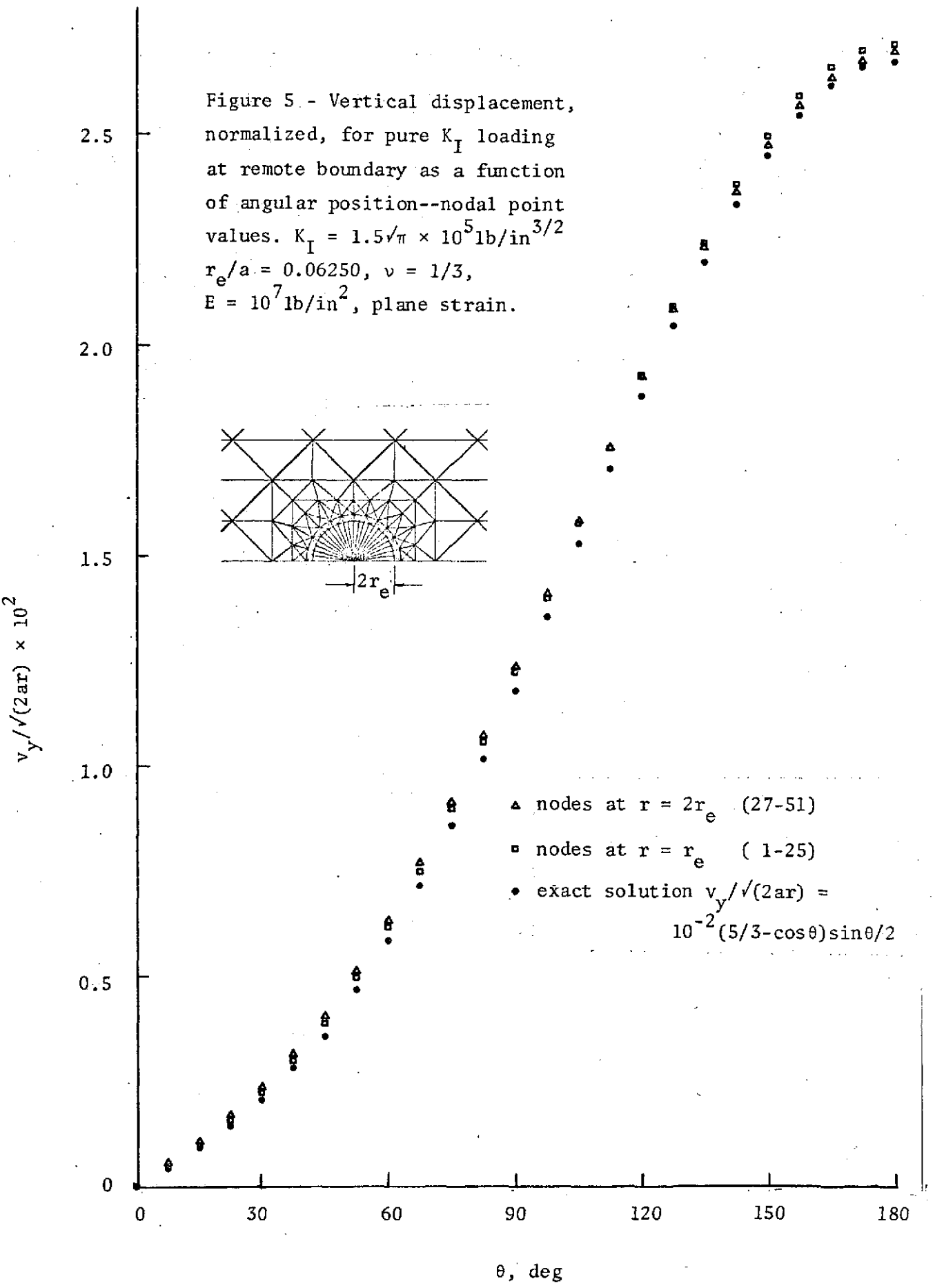

Figure 5 - Vertical displacement, normalized, for pure K_I loading at remote boundary as a function of angular position--nodal point values. $K_I = 1.5\sqrt{\pi} \times 10^5 \text{lb/in}^{3/2}$ $r_e/a = 0.06250$, $\nu = 1/3$, $E = 10^7 \text{lb/in}^2$, plane strain.

Figure 6 - Larger in-plane principal stress, normalized, for pure K_I loading at remote boundary as a function of angular position--element values. $K_I = 1.5\sqrt{\pi} \times 10^5 \text{lb/in}^{3/2}$, $r_e/a = 0.06250$, $Y = 10^5 \text{lb/in}^2$.

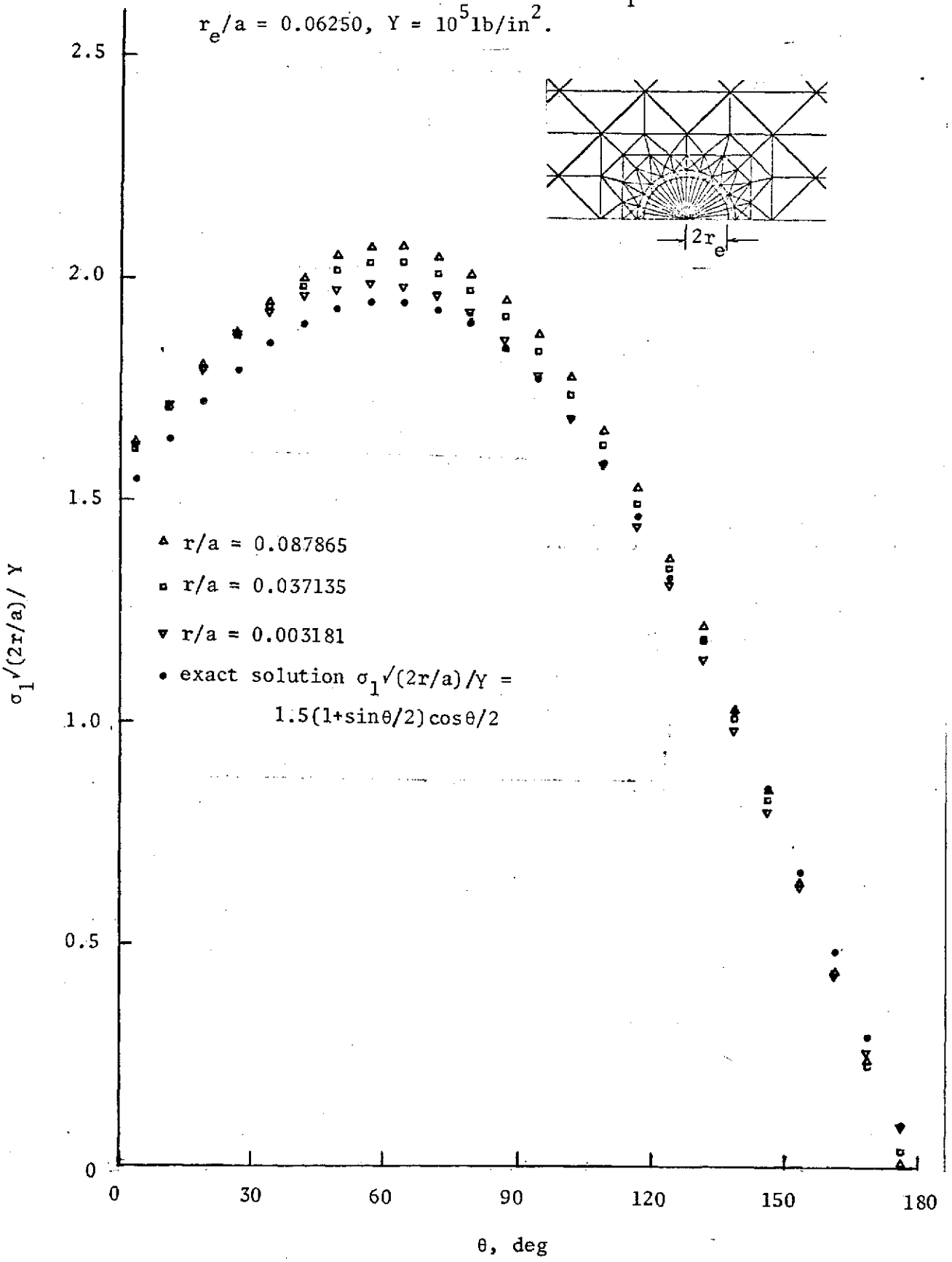

Figure 7 - Smaller in-plane principal stress, normalized, for pure K_I loading at remote boundary as a function of angular position--element values. $K_I = 1.5\sqrt{\pi} \times 10^5 \text{lb/in}^{3/2}$, $r_e/a = 0.06250$, $Y = 10^5 \text{lb/in}^2$.

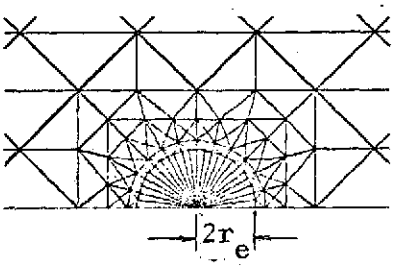

along the flank of the crack.

With indices of performance such as those shown, it is concluded that the elastic response of the program SPECEL is satisfactory. Improvements are accessible through reduction in sector angle, i.e., increase in number of sectors, or through refinements in the interpolation functions (5) or (6). Such improvement, while eventually worth seeking, is separate from the matter of central interest at this stage, namely, how well the overall scheme works.

As an initial foray into this next stage, we adjust the initial loading so that yield is just beyond the point of initiation at the most highly stressed point in the body. For uniform tensile loading this occurs in the twelfth sector and the radial location of the point is $r/a = 0.003181$. The next load increment is set at 5% of the first, the third at 5% of the sum of the first two, and so on. In this manner, loading is built up of a succession of increments [7,10], and we have looked at results for a total of five loading increments.

We observed that both exponents decreased slightly as loading progressed, from the pre-set initial values of 0.5 to $p = 0.402$ and $q = 0.442$. It is reasonable to expect that the exponents should decrease since that implies an increase in the singular nature of the strain increments which, after all, is the sort of behavior accompanying yield. It should be borne in mind that these values of the exponent refer to the displacement increments associated with the fifth load step, *not* to an accumulated value of the respective exponents. We anticipate that, as yield begins, the exponents will change rapidly as the material accomodates the changeover from purely elastic to elasto-plastic response; thereafter the rate at which the exponents change should decline. This pattern of

response characterizes other plane strain analyses we have observed and is discussed at some length in [12].

The second observation made from the initial foray into elasto-plastic response is that the computational time required per load increment is greater than we prefer, about 1 min on the CDC 6600 and over 2 min on the Univac 1108. While such amounts of time are not prohibitive, they are uneconomical and steps are now being taken to reduce the computer requirements for the program to operate.

CONCLUDING REMARKS; A CAVEAT

The formulation of a 'special element' for analysis of elasto-plastic behavior in the vicinity of a crack tip has been outlined, and progress to date summarized. Basically it is evident that the approach is operationally feasible, although certain improvements to code are required before the present program is attractive. Once done, however, the procedure should permit an examination of the *process* of yield in the crack-tip vicinity, taking properly into account the continued presence of elastic strains, plastic strains according to an arbitrary work-hardening stress-strain relationship, unloading, and the sequential nature of the flow process.

It has been noted [13] that an aspect of this approach is open to question, in that the information sought should overlap that already given by the HRR model [4,5], as it is usually termed. The commentary appears to take the following form. If the element size is large with respect to the plastic zone, then the result would be essentially an elastic singularity. Conversely, if the plastic zone is large with respect to the element, the

HRR result should obtain in that it is an asymptotic solution, i.e., it describes behavior within small radial distances from the crack tip. An intermediate situation would perforce give special element results that are some sort of average of the two types of solution. Viewed in another way, this comment suggests that, since the special element is of fixed size in any given analysis, its result in terms, say, of p and q should at most go through a smooth transition from purely elastic values (1/2) to those associated with the HRR results. Hence, there is little to be gained by pursuing this formulation.

Some response to this commentary is in order. There are two aspects to the problem under consideration. One is the (changing) structure of the singularity, and the other is the rate of change it undergoes. The structure is initially that of elasticity and is long since established [14]. It then is altered to something else which, for one somewhat special set of conditions, is also documented [4,5]. Not known, however, is how that second state may be affected by the presence of elastic strains in addition to plastic strains, alternate material behavior (in the sense of the stress-strain curve), and use of flow theory in place of deformation theory as a model of the material. It may be that these factors have but a marginal influence, or they may affect the result to a more pronounced degree. Putting the matter in such simplistic terms, however, begs the second point which may be viewed as concern with the structure of the singularity at any of a sequence of 'intermediate' loads. It is not clear, for example, that the singularity goes monotonically from purely elastic response to 'fully plastic', that there is not some alternation associated with two or three phases of load redistribution as yield and therefore hardening progress. To the extent that such response occurs, it is natural

to expect that both intensity and structure of a singularity will be sensitive to it; none of the information we have seen in the literature reflects this sort of sequencing of events, or process. In spite of the commentary [13], the present work appears worth pursuit, although we stand reminded that sizing the special element is a sensitive matter which bears close examination once we reach the stage of making analyses on a productive basis.

ACKNOWLEDGEMENTS

The work reported above was performed over a period of time at different sites. Sponsorship, therefore, arose from more than one source and, in gratitude, we are pleased to acknowledge them all. During most of the reporting period the author was on leave from Carnegie-Mellon University, and in residence at Imperial College of Science and Technology, London. The respective support of these two institutions, one through its program of faculty leaves and the other through a grant from the (British) Science Research Council, is sincerely appreciated. In addition, the (U.S.) National Aeronautics and Space Administration which, over the years, has provided support for developing the theory of elasto-plastic flow and its applications, has supported this work via Research Grant NGR 39-087-053; such support is particularly valuable and appreciated.

REFERENCES

1. E. Byskov, *International Journal of Fracture Mechanics* 6 (1970) 159-167.

2. W. K. Wilson, in *Stress Analysis and Growth of Cracks* STP 513, American Society for Testing and Materials, Philadelphia (1972) 90-105.

3. P. D. Hilton and J. W. Hutchinson, *Engineering Fracture Mechanics* 3 (1971) 435-451.

4. J. W. Hutchinson, *Journal of the Mechanics and Physics of Solids* 13 (1968) 13-31.

5. J. R. Rice and G. Rosengren, *Journal of the Mechanics and Physics of Solids* 13 (1968) 1-12.

6. D. M. Tracey, On the Fracture Mechanics Analysis of Elasto-Plastic Materials Using the Finite Element Method, Ph.D. Dissertation, Brown University (1973).

7. J. L. Swedlow, A Review of Developments in the Theory of Elasto-Plastic Flow, NASA CR-2321 (1973).

8. O. C. Zienkiewicz, *The Finite Element Method in Engineering Science*, McGraw-Hill, London (1971).

9. R. S. Barsoum, *International Journal of Fracture* 10 (1974) 603-605.

10. J. L. Swedlow, *Computers and Structures* 3 (1973) 879-898.

11. W. F. Brown, Jr. and J. E. Srawley, *Plane Strain Crack Toughness Testing of High Strength Metallic Materials* STP 410, American Society for Testing and Materials, Philadelphia (1966).

12. P. C. Riccardella, An Implementation of the Boundary-Integral Technique for Planar Problems in Elasticity and Elasto-Plasticity, Ph.D. Dissertation, Carnegie-Mellon University (1973).

13. P. C. Paris and J. R. Rice, private communication (1974).

14. M. L. Williams, *Journal of Applied Mechanics* 24 (1957) 109-114.

APPENDIX

ELEMENTS IN MATRICES

Using the abbreviations

$$s_1 = \sin\theta_1 \qquad c_1 = \cos\theta_1$$

$$s_2 = \sin\theta_2 \qquad c_2 = \cos\theta_2$$

The non-zero elements of Q are

$$Q_{11} = Q_{24} = r_e c_1 \qquad Q_{22} = Q_{13} = r_e s_1$$

$$Q_{31} = Q_{44} = 2r_e c_1 \qquad Q_{42} = Q_{33} = 2r_e s_1$$

$$Q_{51} = Q_{64} = 2r_e c_2 \qquad Q_{62} = Q_{53} = 2r_e s_2$$

$$Q_{71} = Q_{84} = r_e c_2 \qquad Q_{82} = Q_{73} = r_e s_2$$

$$Q_{15} = Q_{16}/\theta_1 = r_e^p c_1 \qquad Q_{17} = Q_{18}/\theta_1 = -r_e^q s$$

$$Q_{25} = Q_{26}/\theta_1 = r_e^p s_1 \qquad Q_{27} = Q_{28}/\theta_1 = r_e^q c_1$$

$$Q_{35} = Q_{36}/\theta_1 = 2^p r_e^p c_1 \qquad Q_{37} = Q_{38}/\theta_1 = -2^q r_e^q s_1$$

$$Q_{45} = Q_{46}/\theta_1 = 2^p r_e^p s_1 \qquad Q_{47} = Q_{48}/\theta_1 = 2^q r_e^q c_1$$

$$Q_{55} = Q_{56}/\theta_2 = 2^p r_e^p c_2 \qquad Q_{57} = Q_{58}/\theta_2 = -2^q r_e^q s_2$$

$$Q_{65} = Q_{66}/\theta_2 = 2^p r_e^p s_2 \qquad Q_{67} = Q_{68}/\theta_2 = 2^q r_e^q c_2$$

$$Q_{75} = Q_{76}/\theta_2 = r_e^p c_2 \qquad Q_{77} = Q_{78}/\theta_2 = -r_e^q s_2$$

$$Q_{85} = Q_{86}/\theta_2 = r_e^p s_2 \qquad Q_{87} = Q_{88}/\theta_2 = r_e^q c_2$$

$$Q_{i,9} = Q_{i+1,10} = 1 \quad , \qquad i = 1,3,5,7,9$$

More abbreviations are useful in detailing the elements of [Z]; they are

$$\Delta = \theta_2 - \theta_1 \qquad R = 1/(r_e \sin\Delta)$$

$$P_2 = 1/(2 - 2^p) \qquad R_r = (P_2 - Q_2)R$$

$$Q_2 = 1/(2 - 2^q) \qquad R_1 = R_r s_1 s_2 c_1$$

$$P = P_2/(r_e^p \Delta) \qquad R_2 = R_r s_1 s_2 c_2$$

$$Q = Q_2/(r_e^q \Delta) \qquad R_3 = R_r s_1 c_1 c_2$$

$$R_4 = R_r s_2 c_1 c_2$$

$$\left.\begin{aligned} G_k &= (P_2 c_k^2 + Q_2 s_k^2)R \\ H_k &= (P_2 s_k^2 + Q_2 c_k^2)R \end{aligned}\right\} \quad k = 1,2$$

The non-zero elements of [Z] are given by

$$Z_{11} - Rs_2 = -2Z_{13} = -2G_1 s_2 \qquad -2Z_{15} = Z_{17} + Rs_1 = 2G_2 s_1$$

$$Z_{21} = -2Z_{23} = 2R_3 \qquad -2Z_{25} = Z_{27} = -2R_4$$

$$Z_{31} + Rc_2 = -2Z_{33} = 2G_1 c_2 \qquad -2Z_{35} = Z_{37} - Rc_1 = -2G_2 c_1$$

$$Z_{41} = -2Z_{43} = -2R_1 \qquad -2Z_{45} = Z_{47} = 2R_2$$

$$Z_{51} = -2Z_{53} = 2P\theta_2 c_1 \qquad -2Z_{55} = Z_{57} = -2P\theta_1 c_2$$

$$Z_{61} = -2Z_{63} = -2Pc_1 \qquad -2Z_{65} = Z_{67} = 2Pc_2$$

$$Z_{71} = -2Z_{73} = -2Q\theta_2 s_1 \qquad -2Z_{75} = Z_{77} = 2Q\theta_1 s_2$$

$$Z_{81} = -2Z_{83} = 2Qs_1 \qquad -2Z_{85} = Z_{87} = -2Qs_2$$

$$Z_{12} = -2Z_{14} = -2R_1 \qquad -2Z_{16} = Z_{18} = 2R_2$$

$$Z_{22} + Rc_2 = -2Z_{24} = 2H_1c_2 \qquad -2Z_{26} = Z_{28} - Rc_1 = -2H_2c_1$$

$$Z_{32} = -2Z_{34} = 2R_3 \qquad -2Z_{36} = Z_{38} = -2R_4$$

$$Z_{42} - Rs_2 = -2Z_{44} = -2H_1s_2 \qquad -2Z_{46} = Z_{48} + Rs_1 = 2H_2s_1$$

$$Z_{52} = -2Z_{54} = 2P\theta_2s_1 \qquad -2Z_{56} = Z_{58} = -2P\theta_1s_2$$

$$Z_{62} = -2Z_{64} = -2Ps_1 \qquad -2Z_{66} = Z_{68} = 2Ps_2$$

$$Z_{72} = -2Z_{74} = 2Q\theta_2c_1 \qquad -2Z_{76} = Z_{78} = -2Q\theta_1c_2$$

$$Z_{82} = -2Z_{84} = -2Qc_1 \qquad -2Z_{86} = Z_{88} = 2Qc_2$$

$$\left.\begin{aligned} Z_{j,9} &= -\sum_{n=1}^{4} Z_{j,2n-1} \\ Z_{j,10} &= -\sum_{n=1}^{4} Z_{m,2n} \end{aligned}\right\} \quad j = 1,2,\ldots,8$$

$$Z_{9,9} = Z_{10,10} = 1$$

The interpolation functions $[\alpha(r,\theta)]$ may be written in terms of

$$P_r = Pr^p = (P_2/\Delta)(r/r_e)^p \qquad d_2 = \theta_2 - \theta$$

$$Q_r = Qr^q = (Q_2/\Delta)(r/r_e)^q \qquad d_1 = \theta - \theta_1$$

$$s = \sin\theta \qquad S_2 = \sin d_2$$

$$c = \cos\theta \qquad S_1 = \sin d_1$$

Then

$$\alpha_{11} - RrS_2 = -2\alpha_{13} = -2[G_1rS_2 - P_rd_2c_1c - Q_rd_2s_1s]$$

$$\alpha_{21} = -2\alpha_{23} = -2[R_rrs_1c_1S_2 - P_rd_2c_1s + Q_rd_2s_1c]$$

$$\alpha_{12} = -2\alpha_{14} = -2[R_r r s_1 c_1 s_2 - P_r d_2 s_1 c + Q_r d_2 c_1 s]$$

$$\alpha_{22} - RrS_2 = -2\alpha_{24} = -2[H_1 r S_2 - P_r d_2 s_1 s - Q_r d_2 c_1 c]$$

$$\alpha_{17} - RrS_1 = -2\alpha_{15} = -2[G_2 r S_1 - P_r d_1 c_2 c - Q_r d_1 s_2 s]$$

$$\alpha_{27} = -2\alpha_{25} = -2[R_r r s_2 c_2 S_1 - P_r d_1 c_2 s + Q_r d_1 s_2 c]$$

$$\alpha_{18} = -2\alpha_{16} = -2[R_r r s_2 c_2 S_1 - P_r d_1 s_2 c + Q_r d_1 c_2 s]$$

$$\alpha_{28} - RrS_1 = -2\alpha_{26} = -2[H_2 r S_1 - P_r d_1 s_2 s - Q_r d_1 c_2 c]$$

$$\alpha_{1,9} = 1 - \sum_{n=1}^{4} \alpha_{1,2n-1} \qquad \alpha_{1,10} = -\sum_{n=1}^{4} \alpha_{1,2n}$$

$$\alpha_{2,9} = -\sum_{n=1}^{4} \alpha_{2,2n-1} \qquad \alpha_{2,10} = 1 - \sum_{n=1}^{4} \alpha_{2,2n}$$

Next, let

$$f_1(\theta) = d_1(s^2 + pc^2) - sc \qquad P_r' = P_r/r$$

$$f_2(\theta) = d_2(s^2 + pc^2) + sc \qquad Q_r' = Q_r/r$$

$$g_1(\theta) = (1 - q)d_1 sc - c^2$$

$$g_2(\theta) = (1 - q)d_2 sc + c^2$$

$$h_1(\theta) = 2(1 - p)\Delta sc - h_2(\theta)$$

$$h_2(\theta) = 2(1 - p)d_2 sc + c^2 - s^2$$

$$k_1(\theta) = (1 - q)\Delta(c^2 - s^2) - k_2(\theta)$$

$$k_2(\theta) = (1 - q)d_2(c^2 - s^2) - 2sc$$

So that elements of $[\beta(r,\theta)]$ become

$$\beta_{11} - Rs_2 = -2\beta_{13} = -2\{G_1 s_2 - P_r' c_1 f_2(\theta) + Q_r' s_1[g_2(\theta) - 1]\}$$

$$\beta_{21} = -2\beta_{23} = -2\{-R_3 - P_r' c_1[(1+p)d_2 - f_2(\theta)] - Q_r' s_1 g_2(\theta)\}$$

$$\beta_{31} + Rc_2 = -2\beta_{33} = -2\{-G_1c_2 + R_1 + P_r'c_1h_2(\theta) - Q_r's_1k_2(\theta)\}$$

$$\beta_{12} = -2\beta_{14} = -2\{R_1 - P_r's_1f_2(\theta) - Q_r'c_1[g_2(\theta) - 1]\}$$

$$\beta_{22} + Rc_2 = -2\beta_{24} = -2\{-H_1c_2 - P_r's_1[(1 + p)d_2 - f_2(\theta)] + Q_r'c_1g_2(\theta)\}$$

$$\beta_{32} - Rs_2 = -2\beta_{34} = -2\{H_1s_2 - R_3 + P_r's_1h_2(\theta) + Q_r'c_1k_2(\theta)\}$$

$$\beta_{17} + Rs_1 = -2\beta_{15} = -2\{-G_2s_1 - P_r'c_2f_1(\theta) + Q_r's_2[g_1(\theta) + 1]\}$$

$$\beta_{27} = -2\beta_{25} = -2\{R_4 - P_r'c_2[(1 + p)d_1 - f_1(\theta)] - Q_r's_2g_1(\theta)\}$$

$$\beta_{37} - Rc_1 = -2\beta_{35} = -2\{G_2c_1 - R_2 + P_r'c_2h_1(\theta) - Q_r's_2k_1(\theta)\}$$

$$\beta_{18} = -2\beta_{16} = -2\{-R_2 - P_r's_2f_1(\theta) - Q_r'c_2[g(\theta) + 1]\}$$

$$\beta_{28} - Rc_1 = -2\beta_{26} = -2\{H_2c_1 - P_r's_2[(1 + p)d_1 - f_1(\theta)] + Q_r'c_2g_1(\theta)\}$$

$$\beta_{38} + Rs_1 = -2\beta_{36} = -2\{-H_2s_1 + R_4 + P_r's_2h_1(\theta) + Q_r'c_2k_1(\theta)\}$$

$$\left.\begin{aligned} \beta_{\ell,9} &= -\sum_{n=1}^{4} \beta_{\ell,2n-1} \\ \beta_{\ell,10} &= -\sum_{n=1}^{4} \beta_{\ell,2n} \end{aligned}\right\} \quad \ell = 1,2,3$$

Finally, we note

$$[\gamma(r,\theta)] = \begin{bmatrix} \cos\theta & \sin\theta \\ -\sin\theta & \cos\theta \end{bmatrix} [\alpha(r,\theta)]$$

is the simple transformation required.